

Implementation and Validation of Maximum Power Point Tracking (MPPT) of the Photovoltaic System on Arduino Microcontroller

SALAHEDDINE ZOUIRECH¹, ABDELGHANI EL OUGLI², BELKASSEM TIDHAF¹

¹Embedded Systems, Renewable and Artificial Intelligence Team (SEERIA),
 Mohammed First University, MOROCCO

²Computer Science, Signals, Automation and Cognitivism Laboratory (LISAC),
 Faculty of Sciences, Sidi Mohamed Ben Abdellah University, Fez,
 MOROCCO

Abstract: - In this research paper, we introduce real-time implementation, using Matlab and Simulink environments. The purpose is to study our proposed system, consisting of a photovoltaic, boost converter, and Arduino mega board. The latter communicates with the physical environment from the current and voltage sensors and executes the proposed MPPT commands (perturb-and-observe, short circuit current, incremental conductance, and open circuit voltage), varying the duty cycle of the signal PWM (Pulse Width Modulation) static converter.

Key Words: Photovoltaic system, MPPT, 'P&O' perturb and observe, 'INC' Incremental conductance, short-circuit current (SCC), Open Circuit Voltage (OCV), Arduino Mega, Boost.

Received: August 22, 2021. Revised: August 18, 2022. Accepted: September 17, 2022. Published: October 13, 2022.

1 Introduction

Because of the decrease in fossil energy (oil, gas, etc.) and the fear of growing and invasive pollution, renewable energies (solar, marine, wind, etc.) have become an updated domain, [1], [2].

Photovoltaic energy is a source of renewable energy production based on the solar energy photovoltaic system. In its operation, the photovoltaic generator has non-linear characteristics, which depend on irradiation, and temperature. The adaptation stage is located between the photovoltaic system and the load. The adaptation makes it possible to obtain the photovoltaic system's maximum power, [3], [4].

The main outcome of this work is simulating and practicing the implementation of Perturb and Observe, INC, SCC, and Open Circuit Voltage algorithm, using Arduino Mega board and Matlab / Simulink environment. This framework aims at getting the maximum power of the photovoltaic system regardless of the meteorological conditions vary, [5].

In the beginning, we describe the mathematical model of the photovoltaic cell with more details on the climatic influence conditions on the MPPT. Then, we present how these commands – perturb & observe, short-circuit current, Incremental conductance, and open circuit voltage – function. Afterward, the simulation and experimentation are carried out to recover the maximum power from the

photovoltaic generator by the commands mentioned above. Finally, the paper ends with a conclusion.

2 Photovoltaic Panel

The photovoltaic generator is made of a semiconductor substance; it is formed by different cells connected in parallel or series. These can be schematized by an equivalent circuit that include a single diode as presented in Figure 1, [1], [2], [6], [16], [20], [21].

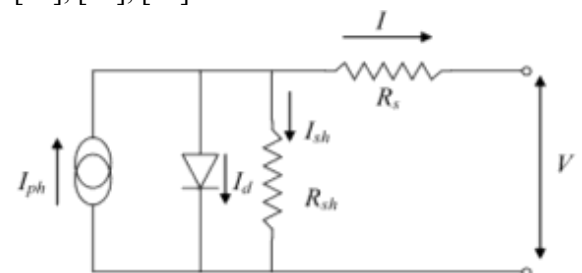


Fig. 1: The equivalent diagram of a photovoltaic cell

The following relation expresses the intensity of the electric current I_{ph} :

$$I_{ph} = \frac{[I_{sc} + K_1(T_c - T_{ref})]G}{G_{ref}} \quad (1)$$

Whereby K_1 is the temperature factor [%/K]; I_{sc} is the short intensity of the electric current [A]; T_c is the panel temperature [K], G is the insolation effect [W/m^2]; $G_{ref} = 1000 W/m^2$ and $T_{ref} = 298 K$.

The relation expressing the electrical current I is:

$$I = I_{ph} - I_d - I_{sh} \quad (2)$$

Whence:

$$I = [I_{sc} + K_f(T_c - T_{ref})] \frac{G}{G_{ref}} - I_s \left[\exp\left(\frac{q(V + R_s I)}{N.K.T} - 1\right) - \frac{(V + R_s I)}{R_{sh}} \right] \quad (3)$$

With:

I_{sc} the short electrical current intensity,
 I_s the electrical current intensity saturation of the diode?

$$I_s = I_{rr} \left(\frac{T}{T_{ref}}\right)^3 \exp\left[qV_g\left(\frac{1}{T_{ref}} - \frac{1}{T}\right)/NK\right] \quad (4)$$

Where E_{rr} is the reverse saturation current at the reference temperature T_{re} , V_g is the bandgap voltage of the semiconductor making up the cell

V the diode tension (V);

q The elementary charge of the electron ($1.60 \cdot 10^{-19}$ C);

K the Boltzmann's universal constant ($1.38 \cdot 10^{-23}$ J/K);

N Ideality factor of the diode,

T the temperature,

R_{ash} is the shunt resistance,

R_s the series resistance,

3 DC-DC Converter Analysis

The converters DC-DC are the main elements of the conversion chain of the photovoltaic generator. They provide interfacing that enables matching between the photovoltaic system and the load to recover the maximum power of the photovoltaic generator, [7], [8], [9], [19], and [20].

The converters consist in most cases of an inductor, a commanded interrupter (using a Metal Oxide Semiconductor Field Effect transistor controlled by a Pulse Width Modulation signal), a capacitor, a diode, linked to a load, [11], [13], and [14].

In this part, we only use the boost converter. The converter boost allows raising the input voltage.

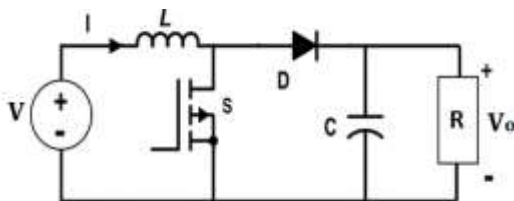


Fig. 2: Boost transformer

The input voltage and output voltage for the converter boost are expressed by:

$$V_0 = \frac{V}{1-D} \quad (5)$$

With D: being the PWM signal duty cycle.

4 Maximum Power Point Tracking (MPPT) Algorithms

The principle of the Maximum Power Point Tracking command is to search the maximum power point by varying the converter duty cycle D, and then bring it to the targeted point. In this paper, we are focused on the usage of four Maximum Power Point Tracking controls: Perturb & observe, short-circuit current (FCC), INC, short-circuit current (FCC), and Open Circuit Voltage (VCO).

4.1 Algorithm Perturb and Observe 'P&O'

The principle of the perturb & observe command is to generate a low-value disturbance of the voltage, which provides a power variation because an increment of the tension electrical leads to an increment of the power, the operating point is to the left of the PPM. If on the opposite the power diminishes, it is right. In the same manner, one can reason for diminished tension. In short, for a disturbance voltage, if the power increment, the direction of the disturbance is maintained. If not, it is reversed so that the operating point tends to the PPM.

The Figure 3 illustrates the flowchart of the perturb & observe control, [6], [8], [10], [11], [12], [13], [15], [17], [18].

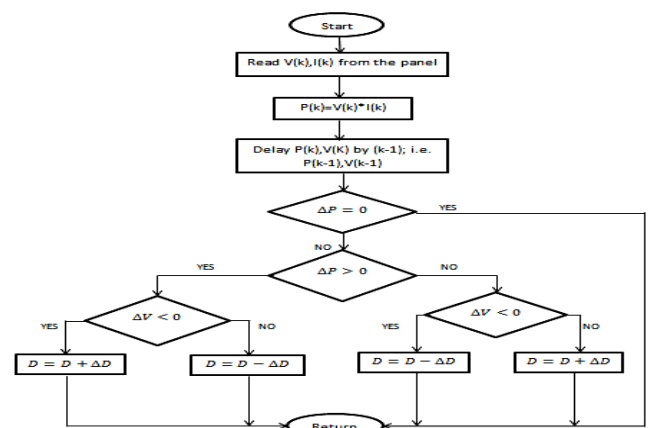


Fig. 3: Flowchart perturb and observe

4.2 Algorithm INC, Increment the Conductance

The flow diagram of INC algorithm is illustrated in Figure 4, [3], [13], [17], [18].

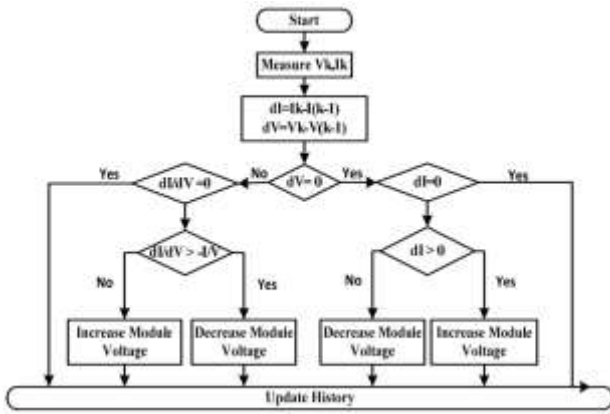


Fig. 4: Flow diagram of INC control

The incremental conductance command is based on the power derivative of the photovoltaic panel about the voltage. This derivative in the PPM point equals zero. We can express this through the following relation:

$$\frac{dP}{dV} = \frac{d(I*V)}{dV} = I + V \frac{dI}{dV} = 0 \quad (6)$$

Giving:

$$\frac{I}{V} = -\frac{dI}{dV} \quad (7)$$

We define the conductance and the increment of the conductance of the source by:

$$G = \frac{I}{V} \text{ et } \Delta G = \frac{dI}{dV} \quad (8)$$

If we place to the right of the maximum power point, we can write:

$$\frac{dP}{dV} < 0 \quad (9)$$

If we place it to the left of the maximum power point, we can write:

$$\frac{dP}{dV} > 0 \quad (10)$$

4.3 Algorithm OCV, Open Circuit Voltage

This control is based on the linear formula between the open circuit voltage and the optimal voltage determined by the following relationship:

$$V_{mpp} = k_1 * V_{oc} \quad (11)$$

Where: V_{mpp} is the photovoltaic generator's maximum output tension electrical and k_1 that varies between 0.73 and 0.8 is a tension electrical coefficient depending on the curve of the photovoltaic panel cell, [5], and [17].

The flow diagram of the OCV method is illustrated in Figure 5

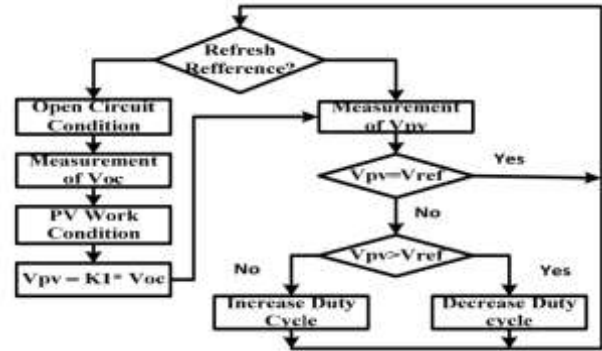


Fig. 5: Flow diagram of OCV control

To achieve the optimum tension electrical, the tension of the open circuit V_{oc} must be determined. As a result, the point of operation of the photovoltaic generator is maintained close to the optimum power point by adjusting the solar generator's tension electrical to the determined optimal tension. The process allows for periodically adjusting of the duty cycle to obtain the optimal voltage electrical.

4.4 Algorithm Short-Circuit Current (SCC)

This control is based on the linear formula between the short-circuit current and the optimal intensity current determined by this equation:

$$I_{mpp} = k_2 * I_{cc} \quad (12)$$

Where k_2 that varies between 0.85 and 0.92 is an intensity of the electric current coefficient depending on the curve of the photovoltaic panel cell, [5], [17].

The flow diagram of SCC control is illustrated in Figure 6.

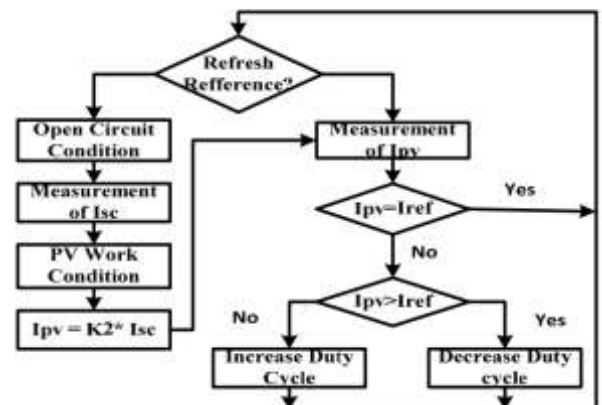


Fig. 6: Flow diagram of SCC control

In reality, the optimal point of operating is reached by taking the intensity of the current electrical of the photovoltaic panel to the optimal current electrical. Thus, the duty cycle is varied until

the photovoltaic generator attains the optimal value, [18].

5 The Simulation Results

The Simulation studies were realized with perturb & observe algorithm, INC, FCC, and VCO, for variable radiation solar and temperature data. Simulation results are obtained in Matlab/Simulink.

We use the diagram below for simulation on Matlab Simulink of the different Maximum Power Point Tracking, methods (perturb & observe, FCC, and VCO).

In the diagram, we present the equivalent diagram of the Boost converter, the photovoltaic panel, and the block that contains the tracking controls.

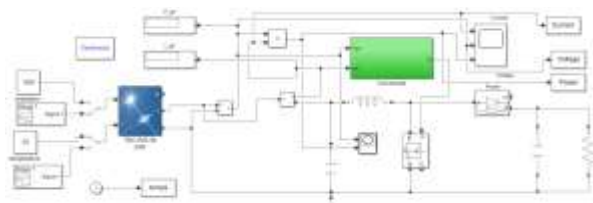


Fig. 7: Block schematic of the photovoltaic generator with P & O, INC, FCC, and FCO commands in Simulink

The figures below show the simulation results for various Maximum Power Point Tracking commands.

Figure 8 presents the power exploiting the different Maximum Power Point Tracking commands: Perturb and Observe, INC, FCC, and FCO for variable irradiation at a constant temperature.

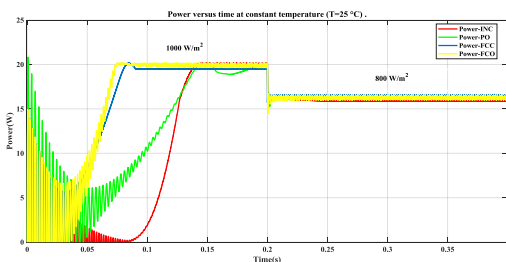


Fig. 8: Power using the different MPPT commands at a constant temperature.

Figure 9 presents the power exploiting the different MPPT commands: Perturb and Observe, INC, FCC, and FCO for a variable temperature at constant irradiation.

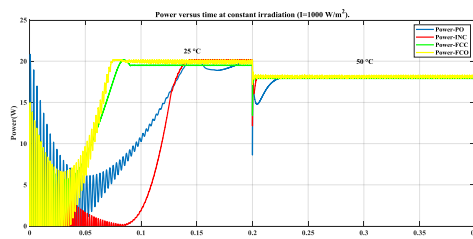


Fig. 9: Power using the different MPPT commands at constant irradiation.

From Figures 8 and 9, we can observe the extraction of the power using the different commands.

6 Practical Part and Results

To validate the MPPT algorithms we propose the following block diagram:

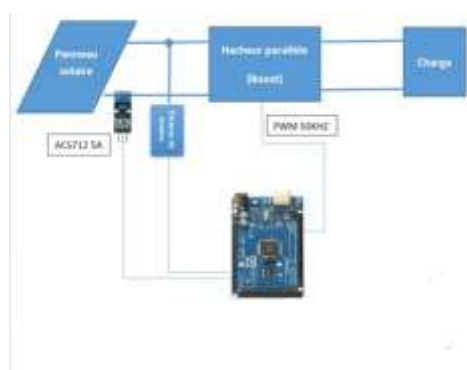


Fig. 10: Synoptic diagram of the realization

Figure 10 shows the block diagram used in this practical part of the photovoltaic system consisting of a 20W photovoltaic system linked to the resistive load by a converter boost connected by a control circuit based on an "Arduino Mega 2560" card which is used. to control the MOSFET transistor of the converter by varying the duty cycle to recover the maximum power at the output of the generator, the output quantities of the panel are measured from two sensors, the first is a tension electrical divider circuit for the measurement of voltage and the second is a current sensor type ACS712 used to determine the current intensity.

All parts have been made and tested separately before assembly.

6.1 The Photovoltaic Panel

In the practical and simulation parts, we use the following photovoltaic generator: TDC-P20-36 of 20W.

Table 1. TDC-P20-36

Open circuit voltage V_{OC}	21,20 V
The voltage at maximum power point V_{mp}	17,20 V
Short-circuit current I_{sc}	1,28 A
Current at maximum power point I_{mp}	1,17 A
Maximum Power	20 W
V_{OC} temperature coefficient	-0.36099 %/deg.C
I_{sc} Temperature coefficient	0.065 %/deg.C

6.2 The ARDUINO Board MEGA 2560 Card

The Arduino Mega board 2560 is an electronic board using the ATmega2560 microcontroller. It includes 54 numeric output/input pins (15 of them have a PWM output), 16 analog inputs, one ceramic (Quartz) resonator at 16 MHz, and one, [3], [8], [12].

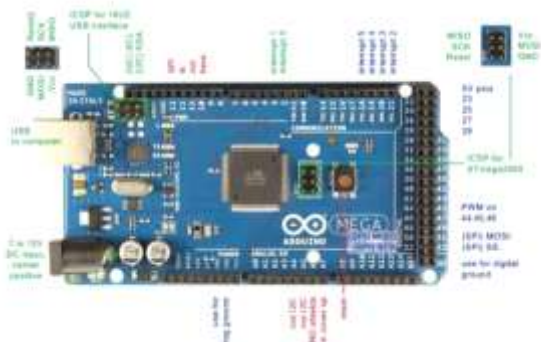


Fig. 11: Arduino Mega

6.3 Current Sensor

ACS712 is used which can detect DC and AC currents. The sensor ACS712 can measure current up to ± 5 A with an output sensitivity of 180 mV / A, [9], [21].

The analog-to-analog-to-digital converter (ADC) reads the values from 0 to 1023. To achieve the value of the intensity of the electric current in a range of 5 A, we use the following relationship:

$$I = \frac{\left(\frac{5}{1023} * \text{Sensore value}\right) - 2.5}{0.185} \quad (13)$$

6.4 Sensor Voltage

The tension electrical measurement is carried out from a tension electrical divider to have a voltage between zero and 5V whatever the value delivered by the photovoltaic panel, [3], [9].

The analog inputs of the Arduino MEGA board can be used to display a DC tension electrical between 0 and 5V.

We consider V_e as the tension electrical to be displayed and V_s as the output voltage of the divider, which will be linked to the entry pin of the Arduino MEGA board. The tension electrical divider lowers the display voltage in the range of the analog inputs of the MEGA Arduino board.

$$V_s = \frac{R_1}{R_1 + R_2} V_e \quad (14)$$

The values of R_1 and R_2 of the sensor are $R_1 = 7,5$ k Ω and $R_2 = 30$ k Ω .

After the previous divisor relation, we must divide the V_s by 1023 and multiply by 5 V to express the real voltage raised by the Arduino MEGA.

Finally, the value of the voltage delivered by the panel is given by the following equation:

$$V = \left(\frac{5}{1023} * \text{Sensore value}\right) * 5 \quad (15)$$

6.5 Optocoupler

The control part must be isolated from the power part. For this, we use the optocoupler. We, therefore, have two very distinct masses on our map. The first: is the mass B.GND, which is the power mass. As well as the A.GND ground which is the control ground and the 5V power supply, [3].

As the Arduino supplies a voltage of 5 volts and the chopper needs a voltage of 15 V to attack the latter, we used the photo coupler type HCPL-3120 to increase the voltage from 5 V to 15V.

The converter boost is placed between a photovoltaic generator and a charge. For a good functioning of the converter it must be controlled by a high frequency (in our case the frequency chooses the order of 7 kHz: to easily filter the output signal and for the correct operation of the converter at 15 V). However, the frequency of the Maximum Power Point Tracking signal delivered by the Arduino MEGA board is limited to a maximum value of 1 kHz so it is necessary to modify the frequency of the Mega Arduino board by the predefined S-function Builder tool in MATLAB Simulink.

The Pulse Width Modulation output signal in the Support Simulink Pack is capped at 490 Hz. This frequency value is not suitable for controlling the converter boost.

To overcome this problem, we use the S-function of MATLAB and a command to raise the Pulse Width Modulation frequency in the Simulink Model.

The command for modifying the Pulse Width Modulation frequency is realized with an S-function

under the Simulink model as illustrated in Figure 12 which presents the unmasking scheme of ‘S-function block’, [3].



Fig. 12: S-Function block

6.6 Experimental Results

The first experimental approach is carried out to determine the Maximum Power Point under the experimental weather data at a given time. If we make the converter’s duty cycle change from 0 to 1, we surely get the maximum power point. To do this, we implement a program on the Arduino Mega board that increments the PWM signal converter duty cycle from 0 to 1 for 30 s. The power supplied by the photovoltaic system is given according to voltage, current, or current according to voltage in Figure 13 during this interval.

Block of test:

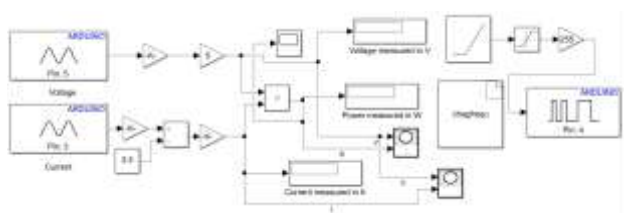


Fig. 13: Block of test

In figures 14, 15, and 16 we can see that the maximum power point in these weather conditions is about 17 W.

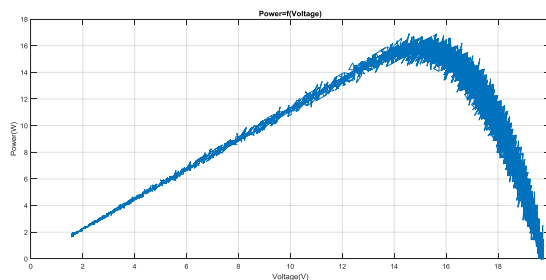


Fig. 14: The variation of the Power according to the Voltage delivered during the first test

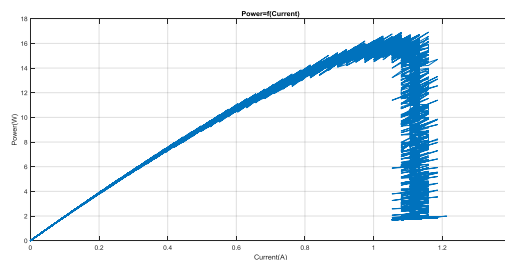


Fig. 15: The variation of the Power according to the Current delivered during the first test

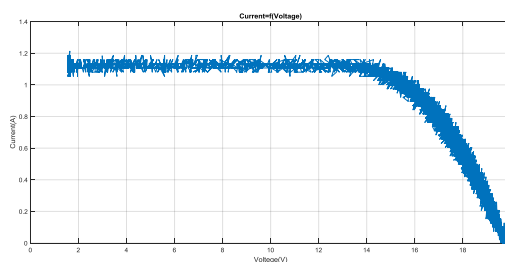


Fig. 16: Current as a function of Voltage delivered during the first test

The second experimental step is to get the maximum power PPM produced by the PV using the different MPPT commands PO, FCC, INC, and VCO under the same conditions as the first test.

The block to recover the power of the photovoltaic system used with the real assembly:

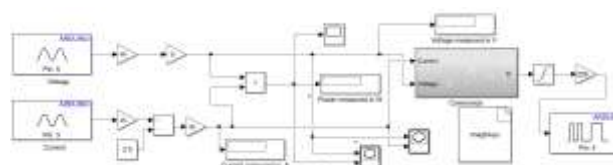


Fig. 17: Block to extract power

Figures 18, 19, 20, and 21 show the power generated by the photovoltaic system using the P&O, INC, FCC, and FCO commands, respectively. Assuming that the weather conditions are unchanged in both experimental steps, the experimental validation of Maximum Power Point Tracking commands can be validated.

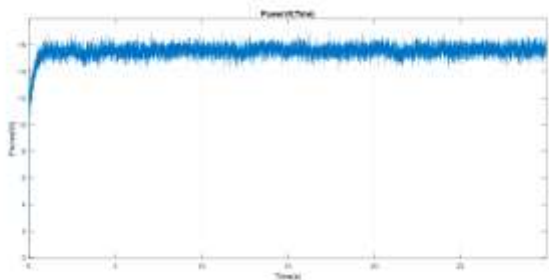


Fig. 18: Power delivered using the P&O algorithm

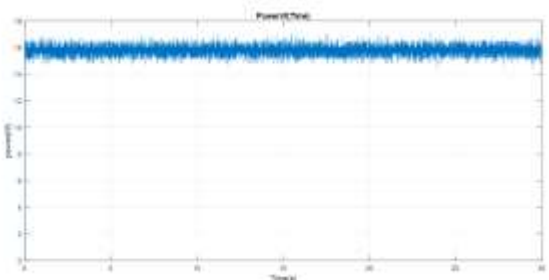


Fig. 19: Power delivered using INC algorithm

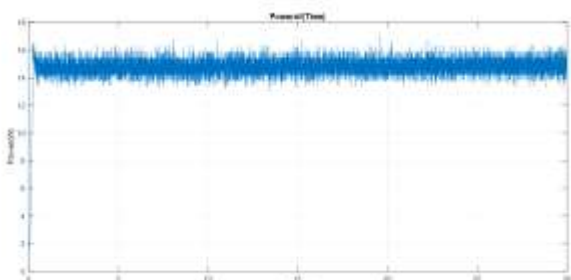


Fig. 20: Power delivered using the FCO algorithm

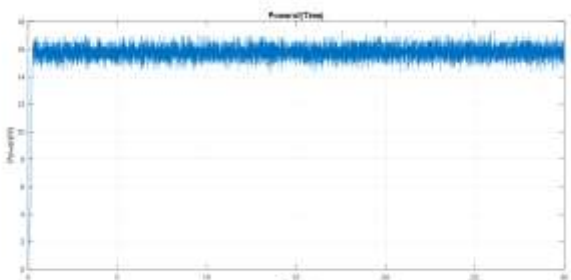


Fig. 21: Power delivered using FCC algorithm

Figures 22, 23, 24, and 25 show the duty cycle using the P&O, INC, FCC, and FCO commands, respectively.

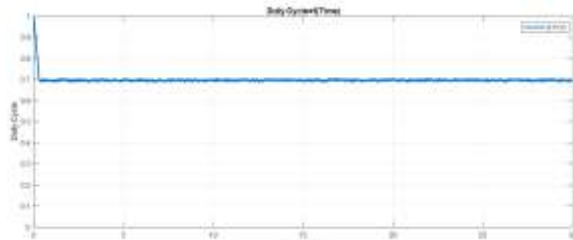


Fig. 22: The duty cycle using FCC

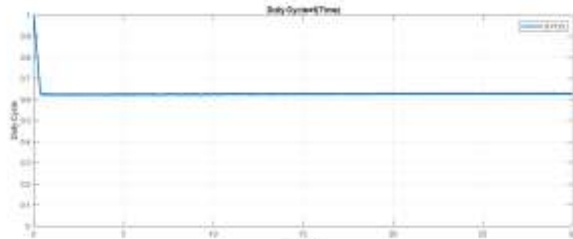


Fig. 23: The duty cycle using FCO

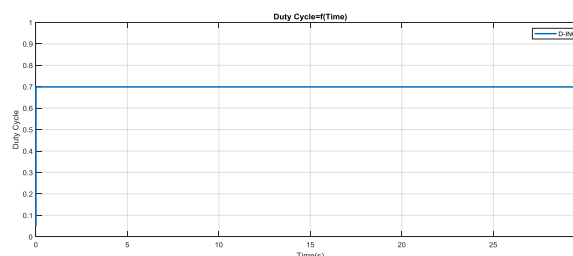


Fig. 24: The duty cycle using INC

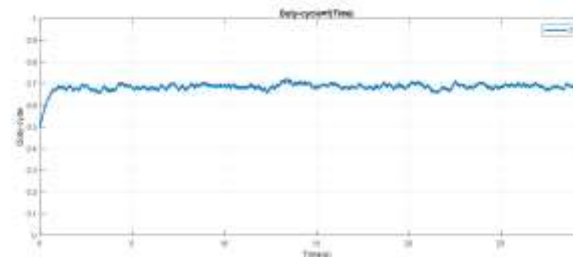


Fig. 25: The duty cycle using P&O

Figures 26, 27, 28, and 29 show the Voltage curves generated by the photovoltaic system using the P&O, INC, FCC, and FCO commands, respectively.

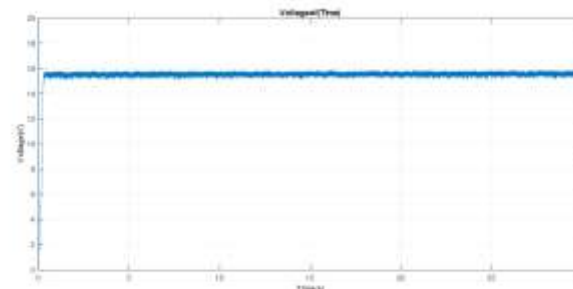


Fig. 26: Voltage delivered using FCC algorithm

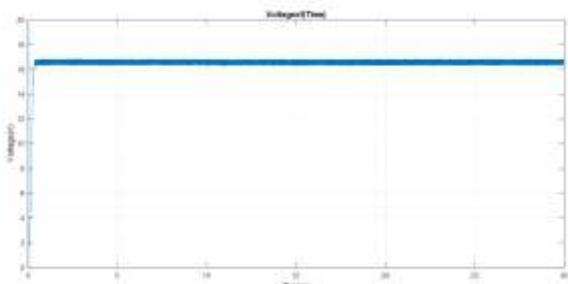


Fig. 27: Voltage delivered using the FCO algorithm

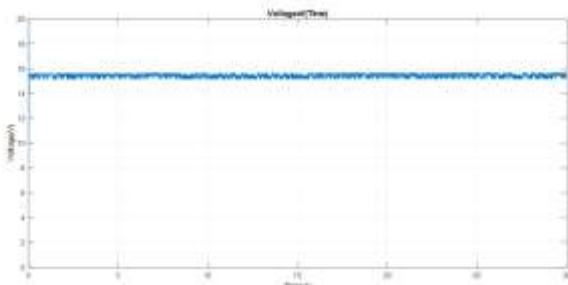


Fig. 28: Voltage delivered using INC algorithm

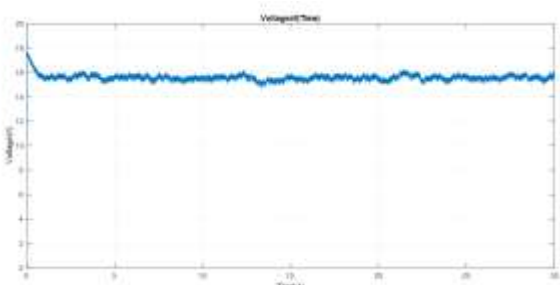


Fig. 29: Voltage delivered using the P&O algorithm

Figures 30, 31, 32, and 33 show the Current curves generated by the photovoltaic system using the P&O, INC, FCC, and FCO commands, respectively.

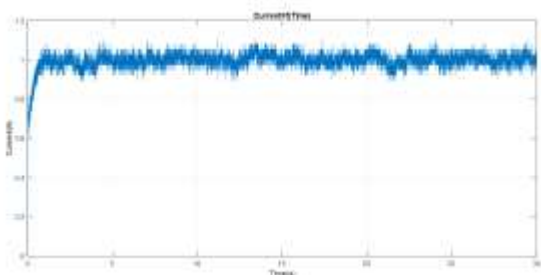


Fig. 30: Current delivered using P&O algorithm

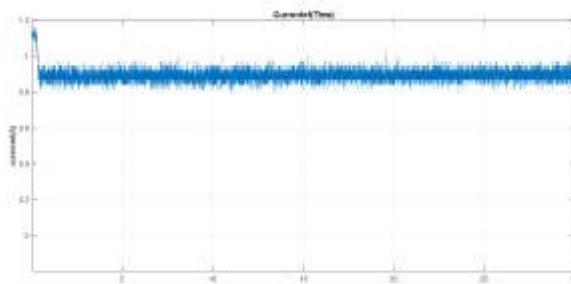


Fig. 31: Current delivered using FCO algorithm

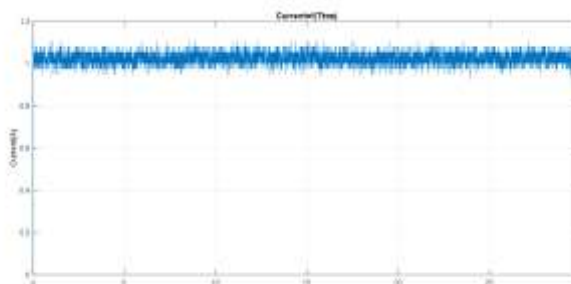


Fig. 32: Current delivered using INC algorithm

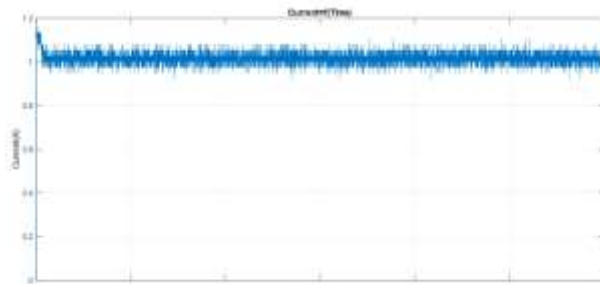


Fig. 33: Current delivered using FCC algorithm

7 Conclusion

This research centers on the use of four MPPT control P&O, INC, VCO, and FCC - to recover the maximum power point from the photovoltaic system. The system was analyzed and designed; the performance was studied by the simulation and experimental implementation. This experiment proves the implementation ability of these commands on the Arduino Mega board for real-time applications.

Moreover, this article proposes a remedy to vary the Pulse Width Modulation frequency of the Mega Arduino board, which provides new perspectives of use with non-dynamic converters. In sum, this article has presented four commands to monitor the MPP of a PV panel.

In future works, we will use the experimental tests of the MPPT, and intelligent methods like fuzzy logic (FL) and Artificial Neural Networks (ANN).

References:

- [1] W. I. Breesam, Real- time implementation of MPPT for renewable energy systems based on Artificial intelligence, International Transactions on Electrical Energy Systems, 2021, p. e12864.
- [2] F. Mhamed, E. Mohamed Larbi, and Z. Smail, Hardware implementation of the fuzzy logic MPPT in an Arduino card using a Simulink support package for PV application, IET Renewable Power Generation, vol. 13, 2019, p. 10-518.
- [3] K. Roshan, N. Geetha, and A. Dalvi, Comparative Study And Implementation Of Incremental Conductance Method And Perturb And Observe Method With Buck Converter By Using Arduino, International Journal of Research in Engineering and Technology, vol. 3, 2014, p. 461- 469.
- [4] J. L. Santos, F. Antunes, A. Chehab, and C. Cruz, A maximum power point tracker for PV systems using a high performance boost converter, solar energy, vol. 80, 2006, p. 772-778.
- [5] S. Motahhir, A. El Hammoumi, and A. El Ghzizal, The most used MPPT algorithms: Review and the suitable low-cost embedded board for each algorithm, Journal of cleaner production, vol. 246, 2020, p. 118983.
- [6] R. Norhasniza Md, N. A. RAHIM, DSP-based maximum peak power tracker using P-O algorithm, IEEE Conference on Clean Energy and Technology (CET), 2011, p. 34-39.
- [7] N. Rouibah, L. Barazane, A. Mellit, A. Hajji, and A. Rabhi, A low-cost monitoring system for maximum power point of a photovoltaic system using IOT technique, International conference on wireless technologies, embedded and intelligent systems (WITS) IEEE, 2019, pp. 1-5.
- [8] O. Nabil, B. Bachir, A. ALLAG , Implementation of a new MPPT Technique for PV systems using a Boost Converter driven by Arduino MEGA, International Conference on Communications and Electrical Engineering (ICCEE). IEEE, 2018, pp. 1-5.
- [9] Y. Ba-khuraissa, A. Al-Hasani, I. Elshafiey, A. F. Sheta, and M. F. Aboud, Experimental implementation of MPPT for PV systems, IEEE 5th International Conference on Electronic Devices, Systems and Applications (ICEDSA), 2016, pp. 1-4.
- [10] E. Mustapha, H. Safa, and F. Sadik, Implementation in Arduino of MPPT using variable step size P-O algorithm in PV installations, International Journal of Power Electronics and Drive Systems, vol. 8, 2017, p. 434.
- [11] R. Alik, and A. Jusoh, An enhanced P-O checking algorithm MPPT for high tracking efficiency of partially shaded PV module, Solar Energy, vol. 163, 2018, pp. 570-580.
- [12] N. C. Swanepoel, C. G. Richards, A. F. Nnachi, and P. J. Ehlers, A comparative study of maximum power point tracking algorithms for PV arrays, IEEE International Energy Conference (ENERGYCon), 2020, pp. 819-823.
- [13] K.Loukil, H. Abbes, H.Abid, M. Abid, and A. Toumi, Design and implementation of reconfigurable MPPT fuzzy controller for photovoltaic systems, in Shams Engineering Journal, vol. 11, 2020, pp. 319-328.
- [14] S. ZOUIRECH, M. ZEROUALI, A. EL O UGLI, and B.Tidhaf, the Impact of the Type of Converter and the Algorithm of the Control on the Production of Maximum Power by a Photovoltaic System IEEE 7th International Renewable and Sustainable Energy Conference, 2019, pp. 1-5.
- [15] W.Xiao, and W. G. Dunford, A modified adaptive hill climbing MPPT method for photovoltaic power systems, IEEE 35th annual power electronics specialists conference, Vol. 3, 2004, pp. 1957-1963.
- [16] S. Zouirech, M. Zerouali, A. El O Ugli, and B.Tidhaf, Application of Various Classical and Intelligent MPPT Tracking Techniques for the Production of Energy through a Photovoltaic System, IEEE 7th International Renewable and Sustainable Energy Conference, 2019, pp. 1-6.
- [17] M. Zerouali, S. Zouirech, A. El O Ugli, and B.Tidhaf, Improvement of Conventional MPPT Techniques P-O and INC by Integration of Fuzzy Logic, IEEE 7th International Renewable and Sustainable Energy Conference, 2019, pp. 1-6.
- [18] M.Boutouba, A.El.Ougli, S.Miqoi and B.Tidhaf, Design and Experimentation of a Control System Implemented on Raspberry Pi 3 Board for Photovoltaic Systems Using SEPIC Converter, Journal of Electrical Systems, vol. 13, 2017, pp. 661-677.
- [19] S. Motahhir, A. El Hammoumi, and A. El Ghzizal, The most used MPPT algorithms: Review and the suitable low-cost embedded

board for each algorithm, Journal of cleaner production, vol. 246, 2020, p. 118983.

- [20] LI, Xingshuo, H. Wen, Y. Hu, Y. Du, and Y. Yang, A comparative study on photovoltaic MPPT algorithms under EN50530 dynamic test procedure, IEEE Transactions on Power Electronics, vol. 36, 2020, pp. 4153-4168.
- [21] S. Gupta, and L. Mathew, Hardware Implementation of Low Cost MPPT using Arduino for PV application, IEEE International Symposium on Sustainable Energy, Signal Processing and Cyber Security, 2020, pp. 1-5.

**Creative Commons Attribution License 4.0
(Attribution 4.0 International, CC BY 4.0)**

This article is published under the terms of the Creative Commons Attribution License 4.0

<https://creativecommons.org/licenses/by/4.0/deed.en>

[US](https://creativecommons.org/licenses/by/4.0/deed.en)